

SMARTINTENTNN:

Towards Smart Contract Intent Detection

Youwei Huang¹, Sen Fang², Jianwen Li^{1,3}, Bin Hu⁴, and Tao Zhang^{5*}

¹ Institute of Intelligent Computing Technology, Suzhou, CAS, China

² North Carolina State University, USA

³ Beijing Normal University - Hong Kong Baptist University United International College, China

⁴ Institute of Computing Technology, Chinese Academy of Sciences, China

⁵ Macau University of Science and Technology, Macao SAR

huangyw@iict.ac.cn, tazhang@must.edu.mo

*Corresponding author

Abstract—Smart contracts on the blockchain offer decentralized financial services but often lack robust security measures, leading to significant economic losses. While substantial research has focused on identifying vulnerabilities in smart contracts, a notable gap remains in evaluating the malicious intent behind their development. To address this, we introduce SMARTINTENTNN (Smart Contract Intent Neural Network), a deep learning-based tool designed to automate the detection of developers’ intent in smart contracts. Our approach integrates a Universal Sentence Encoder for contextual representation of smart contract code, employs a K-means clustering algorithm to highlight intent-related code features, and utilizes a bidirectional LSTM-based multi-label classification network to predict ten distinct categories of unsafe intent. Evaluations on 10,000 real-world smart contracts demonstrate that SMARTINTENTNN surpasses all baselines, achieving an *F1-score* of 0.8633.

A demo video is available at <https://youtu.be/otT0fDYjwK8>.

Index Terms—Web3 Software Engineering, Smart Contract, Intent Detection, Deep Learning

I. INTRODUCTION

A smart contract is a type of computer program and transaction protocol, engineered to execute, control, or document legally binding events and actions automatically according to the stipulations of a contract or agreement [1]. Users generally interact with smart contracts by initiating transactions to invoke various functions. From a programming standpoint, current research on smart contract security predominantly focuses on identifying vulnerabilities and bugs. However, these contracts, while serving as transaction protocols, can be compromised by developers with malicious intent, leading to substantial financial losses.

Figure 1 illustrates several samples of suspicious intent in a real smart contract. All functions share a modifier *onlyOwner*, indicating control by a specific account. For instance, the *onlyOwner* modifier in the *changeTax* function restricts tax fee changes to the development team, while *teamUpdateLimits* allows modifications to transaction limits. Other functions exhibit even more detrimental development intent, permitting the owner to enable or disable the trading function within the smart contract. Unfortunately, current research lacks effective methods for detecting developers’ intent in smart contracts, and manual detection is both time-consuming and costly.

To address the gap in detecting intent in smart contracts, we propose SMARTINTENTNN, an automated deep learning-based tool designed for smart contract intent detection. It integrates a Universal Sentence Encoder (USE) [2] to generate contextual embeddings [3] of smart contracts, a K-means clustering model [4] to identify and highlight intent-related features, and a bidirectional long short-term memory (BiLSTM) [5], [6] multi-label classification network to predict intents in smart contracts. Trained on 10,000 smart contracts and evaluated on another 10,000 distinct contracts, this tool surpasses all baselines, achieving an *F1-score* of 0.8633.

```

function changeTax(
    uint8 buyTax,
    uint8 sellTax
) public onlyOwner {
    _buyTax = buyTax;
    _sellTax = sellTax;
}

function setupEnableTrading() public onlyOwner {
    tradingEnabled = true;
}

function setupDisableTrading() public onlyOwner {
    tradingEnabled = false;
}

function teamUpdateLimits(
    uint256 newBalanceLimit,
    uint256 newSellLimit,
    uint256 newBuyLimit
) public onlyOwner {
    balanceLimit = newBalanceLimit;
    sellLimit = newSellLimit;
    buyLimit = newBuyLimit;
}

```

Fig. 1. Examples of a smart contract with negative intents. BSC address: 0xDDa7f9273a092655a1cF077FF0155d64000ccE2A.

Our contributions are as follows:

- We present the first work on detecting smart contract development intent using deep learning techniques.
- We compile an extensive dataset of over 40,000 smart contracts, labeled with ten categories of intent.
- We open-source the code, dataset, documentation, and models at <https://github.com/web3se-lab/web3-sekit>.

II. DATASET

Since SMARTINTENTNN is implemented with a deep neural network (DNN), we have amassed a dataset of over 40,000 smart contracts sourced from the Binance Smart Chain (BSC) explorer¹. These contracts have been labeled with ten types of intent at the *function* code level. The process involved downloading open-source smart contracts, merging those spanning multiple files, and removing redundant and extraneous code fragments. Finally, we extracted the *function* level code snippets from these contracts.

A. Intent Labels

We categorized the smart contracts in our dataset into ten common intent categories:

- 1 **Fee**: Arbitrarily changes transaction fees, transferring them to specified wallet addresses.
- 2 **DisableTrading**: Enables or disables trading actions on a smart contract.
- 3 **Blacklist**: Restricts designated users' activities, potentially infringing on fair trade rights.
- 4 **Reflection**: Redistributes taxes from transactions to holders based on their holdings, attracting users to buy native tokens.
- 5 **MaxTX**: Limits the maximum number or volume of transactions.
- 6 **Mint**: Issues new tokens, either unlimited or controlled.
- 7 **Honeypot**: Traps user-provided funds under the guise of leaking funds.
- 8 **Reward**: Rewards users with crypto assets to encourage token use, despite possible lack of value.
- 9 **Rebase**: Adjusts token supply algorithmically to control price.
- 10 **MaxSell**: Limits specified users' selling times or amounts to lock liquidity.

The sources of these labels include contributions from StaySafu² as well as insights from decentralized application developers and auditors.

B. Input Extraction

Smart contract source code on BSC can be published either as single-file contracts with merged *imports* or as multiple-file contracts. We consolidate multiple files into a single document.

We remove *pragma* (Solidity compiler version specification), *import* statements, and *comments* as they do not affect intent expression. For multi-file contracts, *import* statements become redundant after merging.

Due to the nature of smart contracts as computer code, direct input into a neural network is impractical. Instead, we use regular expressions to extract *contract*-level and *function*-level code. The *function* code, denoted as \mathcal{F} , is used for model training and evaluation.

III. IMPLEMENTATION

The implementation of SMARTINTENTNN encompasses three primary stages: smart contract embedding, intent highlighting, and multi-label classification learning.

A. Smart Contract Embedding

To embed the context of *functions*, we employ the Universal Sentence Encoder. This embedding process is denoted as $\Phi(\mathcal{F}) : \mathcal{F} \rightarrow \mathbf{f}$, where Φ represents the contextual encoder, and \mathcal{F} denotes the *function* context. The output is a vector \mathbf{f} , which serves as the embedding of the *function* \mathcal{F} .

This embedding process is applied to each *function* within a smart contract. The resultant embeddings, denoted as \mathbf{f} , are aggregated into a matrix \mathbf{X} , which represents the entire smart contract. Specifically, $\mathbf{X} \in \mathbb{R}^{n \times m}$, where n corresponds to the number of *functions* in the smart contract, and m represents the embedding dimension.

B. Intent Highlight

Although it is feasible to directly input \mathbf{X} into a DNN, not all *functions* are relevant to the developer's intent. Therefore, we implement an intent highlight model to extract intent-related *functions* in a smart contract. The highlighting process, denoted as $H(\mathbf{X}) : \mathbf{X} \rightarrow \mathbf{X}'$, utilizes an unsupervised model H to produce intent-highlighted data \mathbf{X}' .

We commence the process by training a K-means clustering model to evaluate the intent strength of each *function* in randomly selecting 1,500 smart contracts. Our experiments reveal that 19 *functions* exhibit frequencies greater than 0.75, indicating common usage among developers. Detailed analysis suggests that these code snippets often originate from public libraries or are sections with high reuse frequency, potentially indicating a weaker developer intent. Conversely, less frequent *functions* tend to express specific and strong developer intent.

To identify *functions* that are significantly distant in spatial distribution from these 19 frequently occurring *functions*, we initially set the number of clusters k to 19 and then conducted a maximum of 80 iterations of K-means clustering training. To compare document similarities, we compute the *cosine distance* between their embedding vectors [7], [8]. Formula 1 defines the cosine similarity between two *functions* (A and B), derived from the cosine of \mathbf{f}^A and \mathbf{f}^B . We then transform the cosine similarity into cosine distance as defined by Formula 2.

$$\cos \langle \mathbf{f}^A, \mathbf{f}^B \rangle = \frac{\mathbf{f}^A \cdot \mathbf{f}^B}{\|\mathbf{f}^A\| \|\mathbf{f}^B\|} \quad (1)$$

$$D(\mathbf{f}^A, \mathbf{f}^B) = 1 - \cos \langle \mathbf{f}^A, \mathbf{f}^B \rangle \quad (2)$$

During training, the K-means model iteratively calculates the cosine distance between centroids and their within-cluster *function* vectors, updating centroids to minimize the total within-cluster variation (TWCV). This iterative process continues until no further significant reduction in TWCV occurs or the maximum iterations are reached. During the training process of K-means clustering, some empty clusters or identical cluster centroids emerged, which were addressed by deleting

¹<https://bscscan.com>

²<https://www.staysafu.org>

or merging them, refining the number of clusters k from 19 to 16. Employing the trained K-means model, the within-cluster distance for each vector f_i can be predicted, which indicates the intent strength—**the greater the distance, the stronger the intent**.

$$X' = H_\mu(X) \text{ by } \mu f_i \text{ if } D(f_i, c_j) \geq \lambda \quad (3)$$

In Formula 3, the feature f_i in matrix \mathbf{X} is scaled by the predicted within-cluster distance to generate a new matrix $\mathbf{X}' \in \mathbb{R}^{n \times m}$, where $i \in \{1, 2, \dots, n\}$ and c_j represents the cluster centroid, $j \in \{1, 2, \dots, 16\}$. Here, $\lambda = 0.21$ is the threshold; beyond it, f_i is scaled by a factor of $\mu = 16$, referred to as H_{16} in Section V. This process amplifies rare *functions*, highlighting their significant intent contribution.

C. Multi-label Classification

In this section, we utilize a DNN model for multi-label binary classification. This model comprises three layers: an input layer, a BiLSTM layer, and a multi-label classification output layer. The matrix X' is fed into the model, which is trained by minimizing 10 combined binary cross-entropy losses corresponding to the 10 intent labels described in Section II.A.

The input layer processes sequences of dimensions $\mathbb{R}^{p \times m}$, where p represents the number of *functions* per time step, and m represents the number of dimensions per *function* embedding. Since the feature dimension is fixed across all embeddings, no modification to the columns of \mathbf{X}' is necessary. It is essential to ensure that m matches the features in \mathbf{f}_i . The row count of \mathbf{X}' varies with the number of *functions* in each smart contract. When \mathbf{X}' has fewer rows than p , meaning $n < p$, the input layer, which also functions as a masking layer with a masking value of zero, pads the missing rows with zero vectors $\mathbf{0}$.

The subsequent layer is a BiLSTM that receives a matrix $X'' \in \mathbb{R}^{p \times m}$ from the input layer. Each LSTM layer comprises p memory cells, totaling $2p$ cells due to the bidirectional configuration. Data is processed through the LSTM's input, forget, and output gates, capturing the semantic context of the smart contract. Let h denote the number of hidden units, and use the vector h to represent the output of a cell. The forward pass generates h^f , and the backward pass yields h^b . The final output of the BiLSTM layer is the concatenation of these vectors, denoted as $h = h^f \oplus h^b$ [9].

$$\mathbf{y} = \text{sigmoid}(\mathbf{W}\mathbf{h} + \mathbf{b}) \quad (4)$$

The output of the BiLSTM layer is ultimately fed into a multi-label classification dense layer. Formula 4 performs binary classification for each intent label using the sigmoid function. The weight matrix W is defined as $W \in \mathbb{R}^{l \times 2h}$, where $2h$ is the size of the input vector h and l is the number of target labels. Consequently, the final output is a vector $y = [y_1, y_2, \dots, y_l]$, where each element represents the probability. The intent detection for the smart contract is now complete.

IV. APPLICATION

We developed SMARTINTENTNN using *Tensorflow.js* [10], creating a web-based tool accessible through any browser. Specifically, SMARTINTENTNN offers two primary modules: intent highlight and intent detection.

A. Intent Highlight

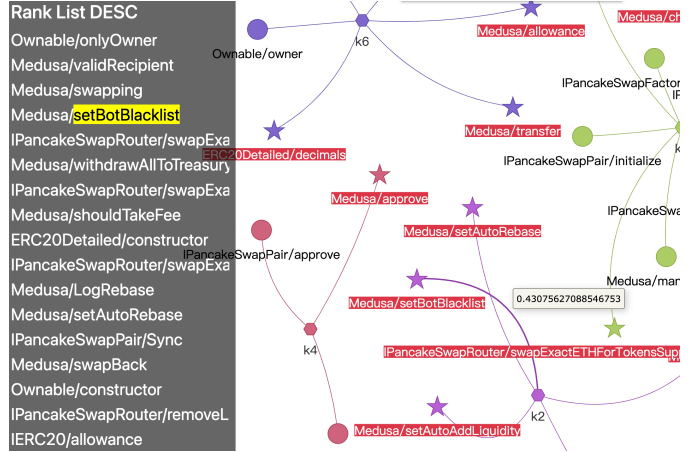


Fig. 2. Example of intent highlighting applied to a smart contract. BSC address: 0xE97CBB39487a4B06D9D1dd7F17f7fBBda4c2b9c4.

The intent highlight feature enables users to swiftly locate *functions* within smart contracts that exhibit specific, strong development intent. In Fig. 2, *functions* exhibiting strong intent are highlighted with a red background. Specifically, a hexagonal node represents the centroid of its corresponding cluster, while a circular node represents a *function* with weak intent and a star represents one with strong intent. When an edge is focused, the distance from the centroid to the *function* is displayed, indicating the strength of the intent. The user interface displays a list of *functions* from a smart contract, ranked by descending intent strength on the left side.

In Fig. 2, several *functions* are highlighted with a red background, such as *setBotBlacklist* and *setAutoRebase*, which indeed exhibit suspicious intent. These *functions* may correspond to the intent categories of **blacklist** and **rebase** described in Section II.A. Non-highlighted *functions* mainly include interfaces or libraries, such as those in *IPancakeSwapPair*.

B. Intent Detection

Our intent detection tool features a text input area that allows users to enter or paste the source code of a smart contract. The tool employs SMARTINTENTNN to predict the intent behind various *functions* in the contract. High-probability intent labels are highlighted in red, distinguishing them from low-probability labels, which are shown in green.

Figure 3 demonstrates that SMARTINTENTNN accurately identified four distinct intents within the analyzed smart contract: **fee**, **disableTrading**, **blacklist**, and **maxTX**. To validate these predictions, we performed an exhaustive manual review of the contract, confirming the existence of the aforementioned intents. Specifically, the **disableTrading** intent is controlled

```
=====
DNN Predict=====
DNN (with BiLSTM) model is loading...
DNN model is predicting intents...
=====
Intents Predicted=====
fee 0.9884564876556396
disableTrading 0.9768874645233154
blacklist 0.9059051275253296
reflect 0.00007938976341392845
maxTX 0.9531305432319641
mint 0.00006963356281630695
honeypot 0.000005496064659382682
reward 0.00008048707968555391
rebase 0.0009889517677947879
maxSell 0.0000011001192206094856
=====
END=====
```

Fig. 3. Illustration of intent detection within a smart contract. BSC address: 0xc4F082963E78deAaC10853a220508135505999E6.

by the *tradingOpen* variable in line 403 and the *tradingStatus* function in line 574, while the **fee**, **maxTX**, and **blacklist** intents are encoded in the code at lines 548 and 552, 544 and 630, and 385 and 681, respectively.

V. EVALUATION

To evaluate SMARTINTENTNN, we employed a confusion matrix to measure key performance metrics, including *accuracy*, *precision*, *recall*, and *F1-score* [11]. In our smart contract intent detection, identifying intent correctly is considered a *True Positive (TP)*, correctly recognizing non-intent scenarios as *True Negative (TN)*, false identifications of intent as *False Positive (FP)*, and missed detections of intent as *False Negative (FN)*. Based on these classifications, we further calculated *accuracy*, *precision*, *recall*, and *F1-score*. The evaluation was conducted on a separate dataset of 10,000 real smart contracts, which was distinct from our training dataset.

This research is pioneering in the field of intent detection in smart contracts and, therefore, has no prior studies for direct comparison. Consequently, we conducted a self-comparison against several established baselines, including models such as LSTM, BiLSTM, and CNN [12]. Furthermore, we benchmarked our model against popular generative large language models (LLMs) for a more comprehensive evaluation.

The evaluation results presented in Table I demonstrate that SMARTINTENTNN with H_{16} outperforms all the baselines and ablation tests, achieving an *F1-score* of 0.8633, an *accuracy* of 0.9647, a *precision* of 0.8873, and a *recall* of 0.8406. This approach markedly surpasses the baselines, with an *F1-score* improvement of 28.14% over LSTM, 14.79% over BiLSTM, 27.80% over CNN, 83.64% over GPT-3.5-turbo, and 63.26% over GPT-4o-mini. We also examined two variants of the intent highlight model: H_2 and the non-highlighted version. The H_2 variant outperformed the non-highlighted version, with this effect being especially evident in the H_{16} model, which underscores the effectiveness of intent highlighting.

TABLE I
BASELINES COMPARISON

Model	Accuracy	Precision	Recall	F1-score
SMARTINTENTNN (Ablation Test)				
USE-H_{16}-BiLSTM	0.9647	0.8873	0.8406	0.8633
USE- H_2 -BiLSTM	0.9581	0.8438	0.8386	0.8412
USE- H_{16} -LSTM	0.9581	0.8731	0.7999	0.8349
USE-BiLSTM	0.9524	0.8337	0.8003	0.8167
USE-LSTM	0.9478	0.8319	0.7587	0.7936
Baseline Models				
LSTM	0.9172	0.7725	0.5973	0.6737
BiLSTM	0.9320	0.7871	0.7200	0.7521
CNN	0.9093	0.6922	0.6596	0.6755
GPT-3.5-turbo	0.8375	0.4135	0.5447	0.4701
GPT-4o-mini	0.7821	0.3703	0.9240	0.5288

VI. CONCLUSION

In this research, we introduced SMARTINTENTNN, a novel automated tool utilizing deep learning models to detect developers' intent in smart contracts. SMARTINTENTNN incorporates a pre-trained USE model, an intent highlight model based on K-means clustering, and a DNN integrated with a BiLSTM layer. Trained on 10,000 and evaluated on another 10,000 distinct smart contracts, SMARTINTENTNN achieved an *F1-score* of 0.8633. The model surpasses all baselines, including the latest generative LLMs.

REFERENCES

- [1] V. Buterin *et al.*, “A next-generation smart contract and decentralized application platform,” *white paper*, vol. 3, no. 37, pp. 2–1, 2014.
- [2] D. Cer, Y. Yang, S.-y. Kong, N. Hua, N. Limtiaco, R. S. John, N. Constant, M. Guajardo-Cespedes, S. Yuan, C. Tar *et al.*, “Universal sentence encoder,” *arXiv preprint arXiv:1803.11175*, 2018.
- [3] T. Mikolov, I. Sutskever, K. Chen, G. S. Corrado, and J. Dean, “Distributed representations of words and phrases and their compositionality,” *Advances in neural information processing systems*, vol. 26, 2013.
- [4] K. Krishna and M. N. Murty, “Genetic k-means algorithm,” *IEEE Transactions on Systems, Man, and Cybernetics, Part B (Cybernetics)*, vol. 29, no. 3, pp. 433–439, 1999.
- [5] S. Hochreiter and J. Schmidhuber, “Long short-term memory,” *Neural computation*, vol. 9, no. 8, pp. 1735–1780, 1997.
- [6] I. Sutskever, O. Vinyals, and Q. V. Le, “Sequence to sequence learning with neural networks,” *Advances in neural information processing systems*, vol. 27, 2014.
- [7] F. Rahutomo, T. Kitasuka, and M. Aritsugi, “Semantic cosine similarity,” in *The 7th international student conference on advanced science and technology ICAST*, vol. 4, no. 1, 2012, p. 1.
- [8] X. Gu, H. Zhang, and S. Kim, “Deep code search,” in *2018 IEEE/ACM 40th International Conference on Software Engineering (ICSE)*. IEEE, 2018, pp. 933–944.
- [9] C. Faith and E. A. Walker, “Direct sum representations of injective modules,” *J. Algebra*, vol. 5, no. 2, pp. 203–221, 1967.
- [10] D. Smilkov, N. Thorat, Y. Assogba, C. Nicholson, N. Kreeger, P. Yu, S. Cai, E. Nielsen, D. Soegel, S. Bileschi *et al.*, “Tensorflow.js: Machine learning for the web and beyond,” *Proceedings of Machine Learning and Systems*, vol. 1, pp. 309–321, 2019.
- [11] Y. Chen, Z. Sun, Z. Gong, and D. Hao, “Improving smart contract security with contrastive learning-based vulnerability detection,” in *Proceedings of the IEEE/ACM 46th International Conference on Software Engineering*, 2024, pp. 1–11.
- [12] Y. LeCun, Y. Bengio *et al.*, “Convolutional networks for images, speech, and time series,” *The handbook of brain theory and neural networks*, vol. 3361, no. 10, p. 1995, 1995.